Original Article
pISSN 1738-2637 / eISSN 2288-2928
J Korean Soc Radiol 2015;72(6):393-400
http://dx.doi.org/10.3348/jksr.2015.72.6.393

대한영상의학회지

Correlation of Magnetic Resonance Imaging Findings of Spinal Intradural Extramedullary Schwannomas with Pathologic Findings[1]

경막내 수외 척수신경초종의 MRI와 조직소견의 비교[1]

Yeo Ju Kim, MD[1], In Suh Park, MD[2], Seung Hwan Yoon, MD[3], Suk Jin Choi, MD[2], Youn Jeong Kim, MD[1], Young-Hye Kang, MD[1], Ha Young Lee, MD[1], Woo Chul Kim, MD[1], Jun Gu Han, MD[1], Soon Gu Cho, MD[1]

Departments of [1]Radiology, [2]Pathology, [3]Neurosurgery, Inha University Hospital, Incheon, Korea

Purpose: To evaluate the magnetic resonance imaging (MRI) findings of spinal intradural extramedullary schwannomas with pathologic correlation and to determine whether these schwannomas share the imaging features of schwannomas in the peripheral nerves.

Materials and Methods: The MRIs of 17 cases of pathologically proven spinal intradural extramedullary schwannomas were reviewed retrospectively, and cystic changes, enhancement, and intratumoral hemorrhage of the tumors were evaluated. Imaging features known to be common findings of schwannoma in the peripheral nerves, such as encapsulation, the target sign, the fascicular sign, and visualization of entering or exiting nerve rootlets, were also evaluated. The histopathology of the tumors was correlated with the MRI findings.

Results: Cystic changes were detected in 14 cases by MRI and in 16 cases by pathology. The most common pattern of enhancement was a thick peripheral septal pattern (70.59%). Intratumoral hemorrhage was detected in four cases on MRI, but in all cases on pathology. Encapsulation was observed in all cases. The fascicular sign was seen in only four cases, and thickening of an exiting rootlet was visualized in one case. None of the cases showed the target sign.

Conclusion: Spinal intradural extramedullary schwannomas were typical encapsulated cystic tumors and had few imaging features of schwannomas in the peripheral nerves.

Index terms
Spinal Intradural Extramedullary Schwannoma
MRI
Pathology

Received December 31, 2014
Accepted April 21, 2015
Corresponding author: In Suh Park, MD
Department of Pathology, Inha University Hospital,
27 Inhang-ro, Jung-gu, Incheon 400-711, Korea.
Tel. 82-32-890-2786 Fax. 82-32-890-2743
E-mail: radzzang@gmail.com

This work was supported by an Inha University Research Grant.

INTRODUCTION

Schwannomas are slow-growing benign tumors of the peripheral nervous system, arising from Schwann cells, and they can occur in any location in the body where peripheral or cranial nerves are present (1). Previous studies reported that schwannomas arising from peripheral nerves frequently present with a fusiform appearance, encapsulation, the target sign (intratumoral peripheral rim of high signal intensity on a T2-weighted image), and the fascicular sign (small ring-like intermediate, low signal intensities with background high signal intensity on a T2-weighted image) on magnetic resonance imaging (MRI) (1, 2). Cystic changes and necrosis can occur, especially in deep-seated large schwannomas of long duration called ancient schwannomas (3). Spinal intradural extramedullary schwannomas are known to have a high frequency of necrosis and cyst formation even when they are small (4). However, most studies of spinal intradural extramedullary schwannomas were case reports or were conducted using low-field MRI in a small number of cases, and their evaluation was therefore limited to radiologic-pathologic correlations (4-7). In addition, we queried whether the imaging findings of peripheral nerve sheath tumors, such as the fascicular sign or the target sign, would be useful in cases of spinal intradural extramedullary schwannomas. The purposes of our study were to

evaluate the correlation between radiologic MRI findings of spinal intradural extramedullary schwannomas and pathologic results, and to determine whether these schwannomas shared the imaging features of their peripheral nerve counterparts.

MATERIALS AND METHODS

This study was approved by our Institutional Review Board. Informed consent was not required for this retrospective study.

Seventeen consecutive cases (nine males and eight females; age range, 34–85 years; mean age, 59.41 years) of pathologically proven intradural extramedullary schwannoma were included in this study between July 2003 and March 2014. All cases underwent an MRI examination before surgical excision. All MRIs were obtained using one of the two 1.5 T MRI machines (SignaHDx, Signa Excite; GE Medical Systems, Milwaukee, WI, USA). Table 1 summarizes the MRI protocols for the cervical, thoracic, and lumbar spine. Contrast-enhanced MRI was carried out within 30 s after the administration of a contrast medium injection of Gadodiamide (Omniscan, 0.2 mmol/kg; GE Healthcare, Princeton, NJ, USA).

Two musculoskeletal radiologists with 6 and 20 years of experience, respectively, reviewed the MRIs and achieved consensus. The MRIs were evaluated with regard to the spinal level, the location relative to the spinal cord, the morphology of the tumor (fusiform, round/ovoid, dumbbell, or lobular shape), enhancement patterns, cystic changes, and intratumoral/extratumoral hemorrhage. The enhancement patterns were classified as homogeneous, heterogeneous, thick peripheral septal (the thicknesses of the peripheral wall and septa were greater than 2 mm), thin peripheral septal (the thicknesses of the peripheral wall and septa were less than 2 mm), central with a peripheral non-enhancing rim, and no enhancement. A cystic change was defined as an area that showed iso-signal intensity to cerebrospinal fluid (CSF) on both T1- and T2-weighted images without enhancement. The area of cystic change was graded as mild (a cystic portion occupying less than one-third of the tumor), moderate (a cystic portion occupying more than one-third but less than two-thirds of the tumor), and severe (a cystic portion occupying more than two-thirds of the tumor). High signal intensities on both T1- and T2-weighted sequences, high signal intensities on a T1-weighted sequence and low signal intensity on a T2-weighted sequence, or dark signal intensities on a T2-weighted sequence within the tumor were regarded as intratumoral hemorrhage. When the signal intensity representing hemorrhage was observed outside the tumor, the location was recorded as the subarachnoid, subdural, and epidural spaces. Imaging features that are known to be the common findings of schwannoma, such as encapsulation, the target sign, the fascicular sign, and visualization of entering or exiting nerve rootlets, were evaluated on a T2-weighted sequence. Encapsulation was defined as the outermost peripheral thin rim of low signal intensity on a T2-weighted sequence. The target sign appeared as a central area of low signal intensity peripherally surrounded by an area of high signal intensity on a T2-weighted image (8). The fascicular sign was defined as multiple small dot-like structures with a higher signal intensity in the background (1, 2, 9). Descriptive analysis was performed for all of the findings.

Pathologic Evaluation

The surgical pathologic specimens of tumors were reviewed by an experienced pathologist for the following findings: the An-

Table 1. MRI Protocols for the Cervical, Thoracic, and Lumbar Spine

	MR Sequences					
	Sag T1	Sag T2	Axial T1	Axial T2	Axial T1 FS with E	Sag T1 FS with E
TR (ms)	600–700	3220	600–700	5000	700–800	700–800
TE (ms)	8–13	123.7	8–13	100	8–13	8–13
ETL	3	16	3	18	3	3
NEX	2	4	2	4	2	2
BW (kHz)	31.25	31.25	31.25	31.25	31.25	31.25
Matrix size	384 × 192	480 × 224	288 × 160	320 × 224	288 × 160	384 × 192
ST/gap (mm)	3/0.3	3/0.3	3/0.1	3/0.1	3/0.1	3/0.3
FOV (mm)	240	240	240	140	140	240

BW = bandwidth, E = enhancement, ETL = echo train length, FOV = field of view, FS = fat saturation, Sag = sagittal, ST = section thickness, TE = echo time, TR = repetition time

toni A and Antoni B areas, cystic changes, intratumoral hemorrhage, hyalinization of vessels, and encapsulation. With the scanning power (12.5 ×) of an Olympus BX microscope, the pathologist looked for any cystic change within the tumor on the pathology slide. The area of cystic change was estimated qualitatively and graded as mild (a cystic portion occupying less than one-third of the tumor), moderate (a cystic portion occupying more than one-third but less than two-thirds of the tumor), and severe (a cystic portion occupying more than two-thirds of the tumor), similar to the MR imaging analysis. When there were multiple areas of cystic change, the total area of cystic change within the tumor was estimated and graded.

RESULTS

Imaging Analysis

As shown in Table 2, more than half of the spinal intradural extramedullary schwannomas developed in the lumbar spine (9/17, 52.94%). Seven schwannomas developed at the level of the cauda equina and 10 schwannomas developed within the spinal cord. Most schwannomas were located posterolaterally (60%, 6/10). The morphology of the tumors was usually lobular (9/17, 52.94%) or round/ovoid (7/17, 41.17%). None of the tumors showed a fusiform morphology. Cystic changes were seen in 14 cases (14/17, 82.35%), of which 10 cases (71.4%) showed severe cystic changes. The most commonly observed enhancement pattern was a thick peripheral septal pattern (12/17, 70.59%) (Fig. 1). All of the non-enhancing areas of the thick peripheral septal enhancing pattern corresponded with the areas of cystic change (Fig. 1). None of the cases showed a thin peripheral septal, central with peripheral non-enhancing rim, or no enhancement pattern. Intratumoral hemorrhage was seen in two cases. Extratumoral hemorrhage was seen in one case, which showed hemorrhage within both the subarachnoid space and the subdural space. Among the common imaging findings of schwannomas in peripheral nerves, encapsulation was the most frequent finding (17/17, 100%). However, the fascicular sign was seen in only four out of the 17 cases (23.52%) and it was not as definite as that in their peripheral counterparts (Fig. 2). Only one case showing thickening of an exiting rootlet was observed (Fig. 2). None of the cases showed the target sign.

Table 2. MRI Findings of Spinal Intradural Extramedullary Schwannomas

Imaging Features	Incidence (n = 17)
Spinal level	
Cervical	1/17 (6%)
Thoracic	7/17 (41.25%)
Lumbar	9/17 (52.94%)
Location relative to the spinal cord (n = 10)	
Ventral	2/10 (20%)
Lateral	2/10 (20%)
Posterolateral	6/10 (60%)
Posterior	0/10 (0%)
Morphology	
Fusiform	0/17 (0%)
Round/ovoid	7/17 (41.12%)
Dumbbell	1/17 (5.8%)
Lobular	9/17 (52.94%)
Enhancement pattern	
Diffuse heterogeneous	3/17 (17.65%)
Diffuse homogeneous	2/17 (11.76%)
Thick peripheral with central non-enhancing portion	12/17 (70.59%)
Thin peripheral with central non-enhancing portion	0/17 (0%)
Central with peripheral non-enhancing rim	0/17 (0%)
No enhancement	0/17 (0%)
Cystic change	14/17 (82.35%)
Mild	0
Moderate	4
Severe	0
Intratumoral hemorrhage	4/17 (23.52%)
Extratumoral hemorrhage	1/17 (6.88%)
Encapsulation	17/17 (100%)
Target sign	0/17 (0%)
Fascicular sign	4/17 (23.52%)
Visualization of entering or exiting rootlet	1/17 (6.88%)

All data are presented as numbers of cases.

Pathologic Analysis

In all cases, the Antoni A and Antoni B areas were mixed and blended imperceptibly, and no demarcation could be discerned between these areas. Areas with cystic change were observed in all but one case (16/17, 94.11%) (Figs. 1, 2). Intratumoral hemorrhage was seen in all cases (Figs. 1, 2). Hyalinization of vessels was seen in 13 out of the 17 cases (76.5%). Encapsulation by the epineurium was seen in all cases.

Correlation between MRI and Pathologic Findings

Correlations between MRI and pathologic findings were found in the cystic changes, intratumoral hemorrhage, and encapsula-

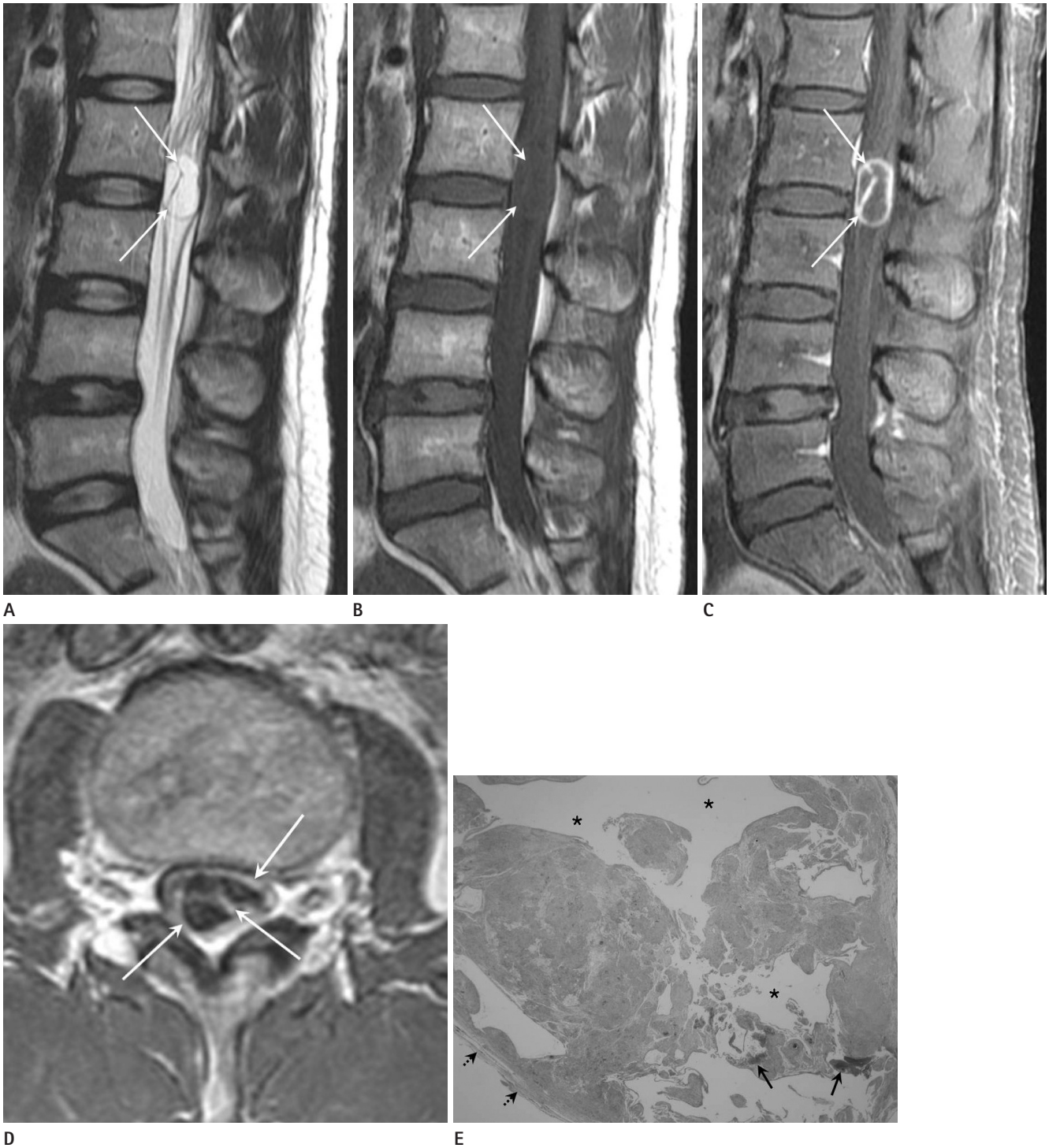

Fig. 1. Sagittal images of T2-weighted **(A)**, T1-weighted **(B)**, fat-suppressed contrast-enhanced T1-weighted sequences **(C)**, axial image of contrast-enhanced T1-weighted sequence, and a photograph **(E)** of pathology in a 49-year-old woman with a spinal intradural extramedullary schwannoma at the level of the L2 vertebral body and L2–3 disc. On the T2-weighted image **(A)**, an intradural extramedullary mass is seen in the thecal sac. The tumor is ovoid in shape with encapsulation (arrows). The signal intensity of the tumor is iso-signal intensity with cerebrospinal fluid on T1- and T2-weighted images **(A, B)** with thick peripheral septal enhancement **(C, D)**, representing cystic changes. The cystic portion occupied more than two-thirds of the tumor (severe cystic changes) on MRI. However, on the photograph of pathology **(E)**, the cystic changes (asterisks) occupied more than one-third but less than two-thirds of the tumor, suggesting moderate cystic changes. The epineurium (dashed arrows in **E**) and intratumoral hemorrhage (arrows) are also seen (hematoxylin and eosin, × 100).

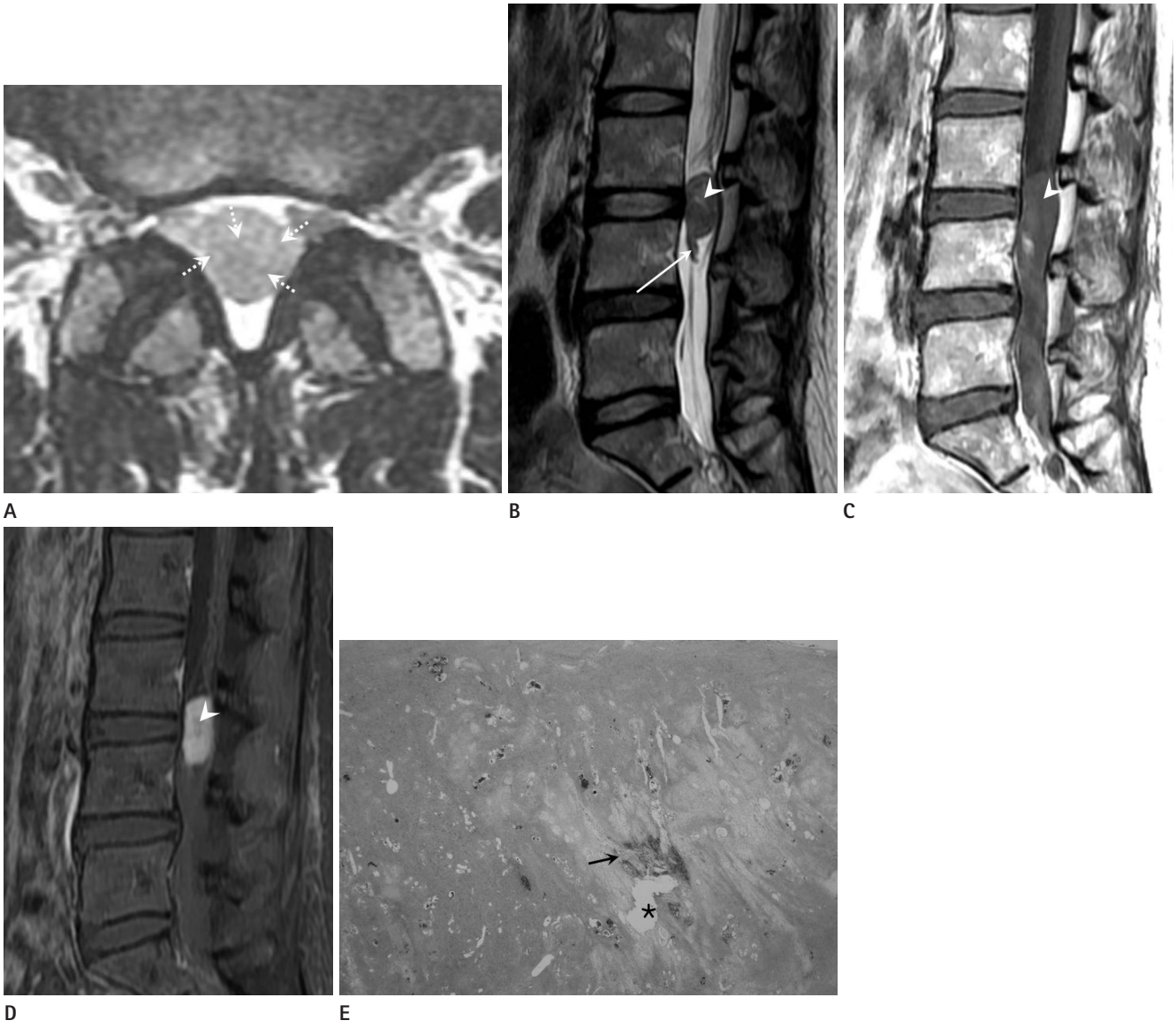

Fig. 2. Axial T2-weighted image **(A)** and sagittal T2-weighted **(B)**, T1-weighted **(C)**, fat-suppressed contrast-enhanced T1-weighted image **(D)**, and photograph **(E)** of pathology (hematoxylin and eosin, × 100) in a 53-year-old woman with a spinal intradural extramedullary schwannoma at the L3–4 disc level. The tumor shows the fascicular sign (dashed arrows in **A**). The exiting cauda equina is thickened (arrow in **B**). A focal ill-defined area showing high signal intensity on the T2-weighted image and iso-signal intensity on the T1-weighted image is seen within the mass (arrowhead in **B**, **C**). It was interpreted as a hypocellular area rather than a cystic lesion because it showed weak enhancement (arrowhead in **D**). No definite cystic changes or hemorrhage is seen on MRI. However, mild cystic changes (asterisk) and hemorrhage (arrow) within the tumor are seen on pathology **(E)**.

tion. Of the ten cases with severe cystic changes on the MRI, half of the cases showed concordant results on pathologic analysis, but in the remaining half of the cases, these changes were underestimated as moderate cystic changes on pathologic analysis. The four cases showing moderate cystic change on MRI showed concordant results on pathologic analysis. Three cases with no definite cystic change on MRI showed mild cystic change on pathologic analysis.

In the pathologic analysis, all of the cases showed hemorrhage within the tumor, but only four cases of intratumoral hemorrhage were evident on MRI. All of the cases showed encapsulation in both the MRI and pathologic findings.

DISCUSSION

Previous studies reported that spinal intradural extramedul-

lary schwannomas most commonly arise from the dorsal sensory roots and usually develop as an asymmetric, well-encapsulated, lobular, firm mass (8, 10, 11). The lumbar region is the most common site for the occurrence of spinal schwannomas (11). All of these findings corresponded well with the results of our study.

In our study, areas with cystic change were seen in more than 82% of the cases on MRI and in 94% of the cases on pathologic analysis. Mild cystic changes determined on pathologic analysis were not seen on MRI. Small areas of high signal intensity within the tumors could hardly be differentiated between hypocellular areas and cystic changes. In contrast, some severe cystic changes seen on MRI were underestimated by pathologic analysis, probably because a cyst can collapse during surgical manipulation and tissue fixation.

The most common enhancement pattern was thick peripheral septal enhancement in our study. All of the non-enhancing areas of the thick peripheral septal enhancing pattern corresponded with the areas of cystic change. According to previous studies (4, 5), peripheral enhancement is not synonymous with cyst formation and necrosis, and may reflect poor central vascularity and/or increased compactness of the tumor with decreased extracellular space available for central accumulation. Sze et al. (5) reported that lesions initially appeared to have peripheral enhancement but they were later filled in on delayed scanning. However, in our study, most of the peripheral enhancement of the spinal intradural extramedullary schwannomas reflected central cystic changes corresponding with the finding in the study by Demachi et al. (6). Friedman et al. (4) assumed that abnormal vascular changes in spinal intradural extramedullary schwannomas resulted in thrombosis and consequently hemorrhage, necrosis, and cyst formation, even in small tumors. Another assumption was that the Antoni B cell area undergoes extensive cystic changes, although they did not recognize any prominence of the Antoni B cell area on pathologic examination (4). In our study, more than 75% of the cases showed hyalinization of the vessels, and all cases had intratumoral hemorrhage. These pathologic results supported the first assumption made by Friedman et al. (4). On pathologic analysis, all of the cases showed intratumoral hemorrhage, but it was evident in only a minority of patients on MRI. Small areas of hemorrhage could hardly be differentiated from the heterogeneous signal intensity of the tumor caused by the heterogeneous mixture of Antoni A and Antoni B areas on MRI. The absence of the gradient sequence, the gold standard for detection of hemorrhage, might decrease the sensitivity for detection of intratumoral hemorrhage.

We also evaluated the imaging features that are known to be common findings in schwannomas of the peripheral nerves, such as encapsulation, the target sign, the fascicular sign, and visualization of entering or exiting nerve rootlets (1, 2). In our study, all of the cases showed encapsulation, representing tumor growth within the epineurium. However, other imaging features suggestive of a benign peripheral nerve sheath tumor, such as the depiction of the nerve entering or exiting the tumor, the target sign, or the fascicular sign, were rarely seen in our study. The depiction of the nerve entering or exiting the tumor is usually seen in peripheral nerve sheath tumors that involve large nerves (1, 9). The structures affected by intradural extramedullary schwannomas are usually thin spinal dorsal sensory rootlets that are difficult to visualize. The entering or exiting affected rootlet can only be seen when it is thickened, as was the case in our study (Fig. 2). The target sign was described in T2-weighted MRI findings of neurogenic tumors (2, 8), which was characterized by a low signal intensity centrally and a high signal intensity peripherally, and it was seen more frequently in neurofibromas (50–70%) than in schwannomas (50%) (2). However, in our study, none of the cases showed the target sign, which was probably related to the frequent cystic changes in schwannomas that were intradural extramedullary in location. The fascicular sign manifests as multiple small ring-like structures with a high signal intensity in the background on T2-weighted images, and is more frequently observed in schwannomas than in neurofibromas (2). Only four cases in our study (23.52%) showed the fascicular sign, but it was not as definite as that in their peripheral counterparts. The absence of the fascicular sign was also probably related to the frequent cystic changes in spinal intradural extramedullary schwannomas.

Differential diagnoses of spinal intradural extramedullary schwannomas include other intradural extramedullary tumors, nontumorous intradural extramedullary cysts, and parasitic infestations. Neurofibroma, another type of benign nerve sheath tumor, usually presents as a solid mass showing the target sign, in contrast to the intradural extramedullary schwannoma (4). Meningioma, the second most common intradural extramedullary tumor, shows intense and uniform enhancement and intratumoral

cysts are very rare (12). The dural tail sign and calcifications are more frequently seen in meningioma than in intradural extramedullary schwannoma (12, 13). Myxopapillary ependymoma, a distinct clinicopathologic variant of ependymoma, is observed exclusively in the conus medullaris and filum terminale, and it typically manifests as a huge sausage-shaped mass with intense enhancement (13). Paragangliomas are also found in the conus medullaris, cauda equina, or filum terminale and present as inhomogeneous, highly vascular solid masses (13), for which intratumoral and adjacent vessels with flow voids are a prerequisite (13).

Non-tumorous intradural extramedullary cysts, such as dermoid cysts, epidermoid cysts, arachnoid cysts, and enterogenous cysts, should also be differentiated from the severe cystic changes of spinal intradural extramedullary schwannomas. Dermoid cysts are diagnosed easily because of their fat content (14, 15). Epidermoid cysts show various characteristics on MRI but they usually show signal intensity similar to that of CSF on T1- and T2-weighted sequences. They can have a thin or slightly thick peripheral capsule with or without enhancement (15). On diffusion weighted MRI, the epidermoid cyst shows restricted diffusion due to its keratin content in contrast to the severe cystic changes of spinal intradural extramedullary schwannomas (16). Presence of dermal sinus tract or other spinal dysraphism can be helpful in the diagnosis of both dermoid and epidermoid cysts (15). Intradural arachnoid cysts unusually arise from the region of the septum posticum at the thoracic level and have an extremely thin wall without enhancement (17). Enterogenous cysts are likely to develop anteriorly and be confined to the cervical region (17). Usually, their walls are very thin and not enhanced.

Cystic lesions caused by parasitic infestations can also be confused with the severe cystic changes of spinal intradural extramedullary schwannomas. The subarachnoid form of cysticercosis may manifest as intradural extramedullary cysts with or without diffuse arachnoiditis (18). Intracystic scolex formation and concomitant intracranial involvement can be used as diagnostic clues (18). Hydatid cysts have a characteristic imaging feature of two dome-shaped ends with no debris in the lumen, resembling a sausage on MRI (19).

The major limitation of this study is that it was retrospective analysis. We did not perform any statistical analysis. The study population comprised only 17 cases and the sample size was too small to generalize the results. However, this is the largest study to evaluate the correlation of MRI findings of spinal intradural extramedullary schwannoma with pathologic findings.

In conclusion, spinal intradural extramedullary schwannomas were typically encapsulated lobular cystic tumors and had few imaging features of benign peripheral nerve sheath tumors; therefore, the imaging findings of the latter entity may not be helpful.

REFERENCES

1. Murphey MD, Smith WS, Smith SE, Kransdorf MJ, Temple HT. From the archives of the AFIP. Imaging of musculoskeletal neurogenic tumors: radiologic-pathologic correlation. *Radiographics* 1999;19:1253-1280
2. Jee WH, Oh SN, McCauley T, Ryu KN, Suh JS, Lee JH, et al. Extraaxial neurofibromas versus neurilemmomas: discrimination with MRI. *AJR Am J Roentgenol* 2004;183:629-633
3. Isobe K, Shimizu T, Akahane T, Kato H. Imaging of ancient schwannoma. *AJR Am J Roentgenol* 2004;183:331-336
4. Friedman DP, Tartaglino LM, Flanders AE. Intradural schwannomas of the spine: MR findings with emphasis on contrast-enhancement characteristics. *AJR Am J Roentgenol* 1992;158:1347-1350
5. Sze G, Bravo S, Krol G. Spinal lesions: quantitative and qualitative temporal evolution of gadopentetate dimeglumine enhancement in MR imaging. *Radiology* 1989;170(3 Pt 1):849-856
6. Demachi H, Takashima T, Kadoya M, Suzuki M, Konishi H, Tomita K, et al. MR imaging of spinal neurinomas with pathological correlation. *J Comput Assist Tomogr* 1990;14:250-254
7. Borges G, Bonilha L, Proa M Jr, Fernandes YB, Ramina R, Zanardi V, et al. Imaging features and treatment of an intradural lumbar cystic schwannoma. *Arq Neuropsiquiatr* 2005;63:681-684
8. Koga H, Matsumoto S, Manabe J, Tanizawa T, Kawaguchi N. Definition of the target sign and its use for the diagnosis of schwannomas. *Clin Orthop Relat Res* 2007;464:224-229
9. Kransdorf M, Murphey MD. *Neurogenic tumors.* In Kransdorf MJ, Murphey MD. *Imaging of soft tissue tumors.* Phil-

adelphia, PA: Saunders, 1997:235-273
10. Katonis P, Kontakis G, Pasku D, Tzermiadianos M, Tzanakakis G, Hadjipavlou A. Intradural tumours of the lumbar spine presenting with low back pain: report of two cases and review of the literature. *Acta Orthop Belg* 2008;74:282-288
11. Conti P, Pansini G, Mouchaty H, Capuano C, Conti R. Spinal neurinomas: retrospective analysis and long-term outcome of 179 consecutively operated cases and review of the literature. *Surg Neurol* 2004;61:34-43; discussion 44
12. De Verdelhan O, Haegelen C, Carsin-Nicol B, Riffaud L, Amlashi SF, Brassier G, et al. MR imaging features of spinal schwannomas and meningiomas. *J Neuroradiol* 2005;32:42-49
13. Van Goethem JW, van den Hauwe L, Ozsarlak O, De Schepper AM, Parizel PM. Spinal tumors. *Eur J Radiol* 2004;50:159-176
14. Mhatre P, Hudgins PA, Hunter S. Dermoid cyst in the lumbosacral region: radiographic findings. *AJR Am J Roentgenol* 2000;174:874-875
15. Thompson DN. Spinal inclusion cysts. *Childs Nerv Syst* 2013;29:1647-1655
16. Teksam M, Casey SO, Michel E, Benson M, Truwit CL. Intraspinal epidermoid cyst: diffusion-weighted MRI. *Neuroradiology* 2001;43:572-574
17. Matsui H, Kanamori M, Yudoh K, Ohmori K, Yasuda T, Wakaki K. Cystic spinal cord tumors: magnetic resonance imaging correlated to histopathological findings. *Neurosurg Rev* 1998;21:147-151
18. Leite CC, Jinkins JR, Escobar BE, Magalhães AC, Gomes GC, Dib G, et al. MR imaging of intramedullary and intradural-extramedullary spinal cysticercosis. *AJR Am J Roentgenol* 1997;169:1713-1717
19. Güneçs M, Akdemir H, Tuğcu B, Günaldi O, Gümüçs E, Akpinar A. Multiple intradural spinal hydatid disease: a case report and review of literature. *Spine (Phila Pa 1976)* 2009;34:E346-E350

경막내 수외 척수신경초종의 MRI와 조직소견의 비교[1]

김여주[1] · 박인서[2] · 윤승환[3] · 최석진[2] · 김윤정[1] · 강영혜[1] · 이하영[1] · 김우철[1] · 한준구[1] · 조순구[1]

목적: 경막내 수외 척수신경초종의 MRI 소견과 조직학적 소견을 비교하고 말초신경초종과 영상소견을 공유하는지 알아보고자 하였다.

대상과 방법: 조직학적으로 확진된 17 증례의 경막내 수외 척수신경초종의 수술 전 MRI를 이용하여 조영증강, 낭종성 변화, 종양내출혈 및 말초신경초종의 흔한 영상소견인 피막형성, 과녁징후, 다발징후, 들어가고 나가는 신경근이 보이는지에 대해 후향적으로 분석하고 조직학적 소견과 비교했다.

결과: MRI에서는 14 증례가, 병리조직에서는 16 증례가 낭종성 변화를 보였다. 가장 흔한 조영증강 유형은 두꺼운 변연/격막 조영증강이었다(70.59%). 종양내 출혈은 MRI에서는 4 증례에서만 보였으나 병리조직에서는 모두 관찰되었다. 피막형성은 MRI와 병리의 모든 증례에서 보였고, 다발징후는 4예, 들어가고 나가는 신경근은 1예만 MRI에서 관찰되었다. 과녁징후는 모든 증례에서 보이지 않았다.

결론: 경막내 수외 척수신경초종은 피막에 싸여진 낭성 종양으로 보이는 경우가 흔하며 말초신경초종의 전형적 영상소견은 거의 보이지 않는다.

인하대학교병원 [1]영상의학과, [2]병리과, [3]신경외과